American Journal of Case Reports

e-ISSN 1941-5923
© Am J Case Rep, 2026; 27: e954845
DOI: 10.12659/AJCR.954845

Received: 2026.07.15
Accepted: 2026.10.08
Available online: 2026.11.16
Published: 2026.XX.XX

SFPQ/PSF-TFE3 Renal Cell Carcinoma Mimicking TFEB-Rearranged Renal Cell Carcinoma and Co-Occurring With High-Grade Urothelial Carcinoma: A Case Report

Authors' Contribution:
Study Design A
Data Collection B
Statistical Analysis C
Data Interpretation D
Manuscript Preparation E
Literature Search F
Funds Collection G

BEF 1 Xin Zhou
EF 2 Corbin J. Eule
EF 3 Janet Kukreja
ABEF 1 Frances Xiuyan Feng

1 Department of Pathology, University of Colorado Anschutz Medical Campus, Aurora, CO, USA
2 Department of Medicine, Division of Medical Oncology, University of Colorado Anschutz Medical Campus, Aurora, CO, USA
3 Division of Urology, University of Colorado Anschutz Medical Campus, Aurora, CO, USA

Corresponding Author: Frances Xiuyan Feng, 12631 East 17th Avenue, Aurora, CO 80045, USA
Phone: 720-848-8940, e-mail: frances.feng@cuanschutz.edu

Financial support: None declared
Conflict of interest: None declared

APPROVED GALLEY PROOF

Patient: Female, 66-year-old
Final Diagnosis: Renal cell carcinoma • SFPQ/PSF-TFE3 renal cell carcinoma
Symptoms: Hematuria • recurrent urinary tract infections • urinary urgency • weight loss
Clinical Procedure: —
Specialty: Pathology

Objective: Rare disease

Background: Transcription factor E3 (TFE3)-rearranged renal cell carcinoma is a rare subtype of renal tumor that relatively more frequent in the pediatric population. Histologically, it typically presents as a papillary neoplasm composed of clear epithelial cells with numerous psammoma bodies. Transcription factor EB (TFEB)-rearranged renal cell carcinoma is an even rarer entity, classically characterized by biphasic cellular morphology, rosette-like structures, and eosinophilic basement membrane-like material.

Case Report: We describe a case of splicing factor proline- and glutamine-rich (SFPQ)/polypyrimidine tract-binding protein-associated splicing factor (PSF)-TFE3 renal cell carcinoma confirmed by RNA sequencing that morphologically mimicked TFEB-rearranged renal cell carcinoma in a 66-year-old woman with concurrent high-grade urothelial carcinoma of the urinary bladder and ureter.

Conclusions: This case expands the recognized histologic spectrum of TFE3-rearranged renal cell carcinoma and highlights the critical role of molecular testing in establishing a definitive diagnosis.

Keywords: SFPQ/PSF-TFE3 • TFEB • Renal Cell Carcinoma • Urothelial Carcinoma

Full-text PDF: https://www.amjcaserep.com/abstract/index/idArt/954845

2064 — 3 15

Publisher's note: All claims expressed in this article are solely those of the authors and do not necessarily represent those of their affiliated organizations, or those of the publisher, the editors and the reviewers. Any product that may be evaluated in this article, or claim that may be made by its manufacturer, is not guaranteed or endorsed by the publisher

This work is licensed under Creative Commons Attribution-NonCommercial-NoDerivatives 4.0 International (CC BY-NC-ND 4.0)

Indexed in: [PMC] [PubMed] [Emerging Sources Citation Index (ESCI)] [Web of Science by Clarivate]

APPROVED GALLEY PROOF

Introduction

Microphthalmia-associated transcription factor family translocation renal cell carcinoma (MiT-RCC) is a rare subtype of renal cell carcinoma (RCC), representing approximately 1% of all RCCs and one-third of pediatric RCCs [1]. In the 2016 World Health Organization (WHO) Classification (4th edition) [2], MiT-RCC included 2 subtypes: transcription factor E3 (TFE3)-rearranged RCC and transcription factor EB (TFEB)-rearranged RCC. TFE3-rearranged RCC is caused by Xp11.2 translocations, whereas TFEB-rearranged RCC harbors fusions involving the gene that encodes the TFEB transcription factor through a t(6;11) translocation.

Through advances in molecular testing, TFEB-amplified RCC has also been recognized. This subtype exhibits amplification of the 6p21 locus harboring TFEB, resulting in TFEB overexpression and its downstream effects. Consequently, TFEB-amplified RCC and TFEB-rearranged RCC are now considered 2 subtypes of TFEB-altered RCC. In the current WHO Classification (5th edition), TFEB-altered RCC, along with TFE3-rearranged RCC and other RCCs exhibiting specific genetic alterations, is classified as molecularly defined RCC [3].

Although most MiT-RCCs have a prominent clear cell component and may be morphologically confused with clear cell RCC, immunohistochemical staining panels have been established to differentiate MiT-RCC from other, more common RCC subtypes [4]. In rare cases, TFE3-rearranged RCC cannot be distinguished from TFEB-rearranged RCC based solely on morphological features because of overlap between these 2 entities [5,6]. Here, we report a case of TFE3-rearranged RCC that closely mimicked TFEB-rearranged RCC morphologically and co-occurred with high-grade urothelial carcinoma of the ureter and urinary bladder. The diagnosis was ultimately established through molecular testing, highlighting the importance of molecular studies in diagnostically challenging cases.

Case Report

A 66-year-old Asian American woman presented to our hospital with gross hematuria, urinary urgency, recurrent urinary tract infections, and unintentional weight loss over the preceding 3 months. She was a smoker (0.3 packs/day for 40 years) without a notable medical or surgical history or family history of cancer. Abdominopelvic computed tomography intravenous

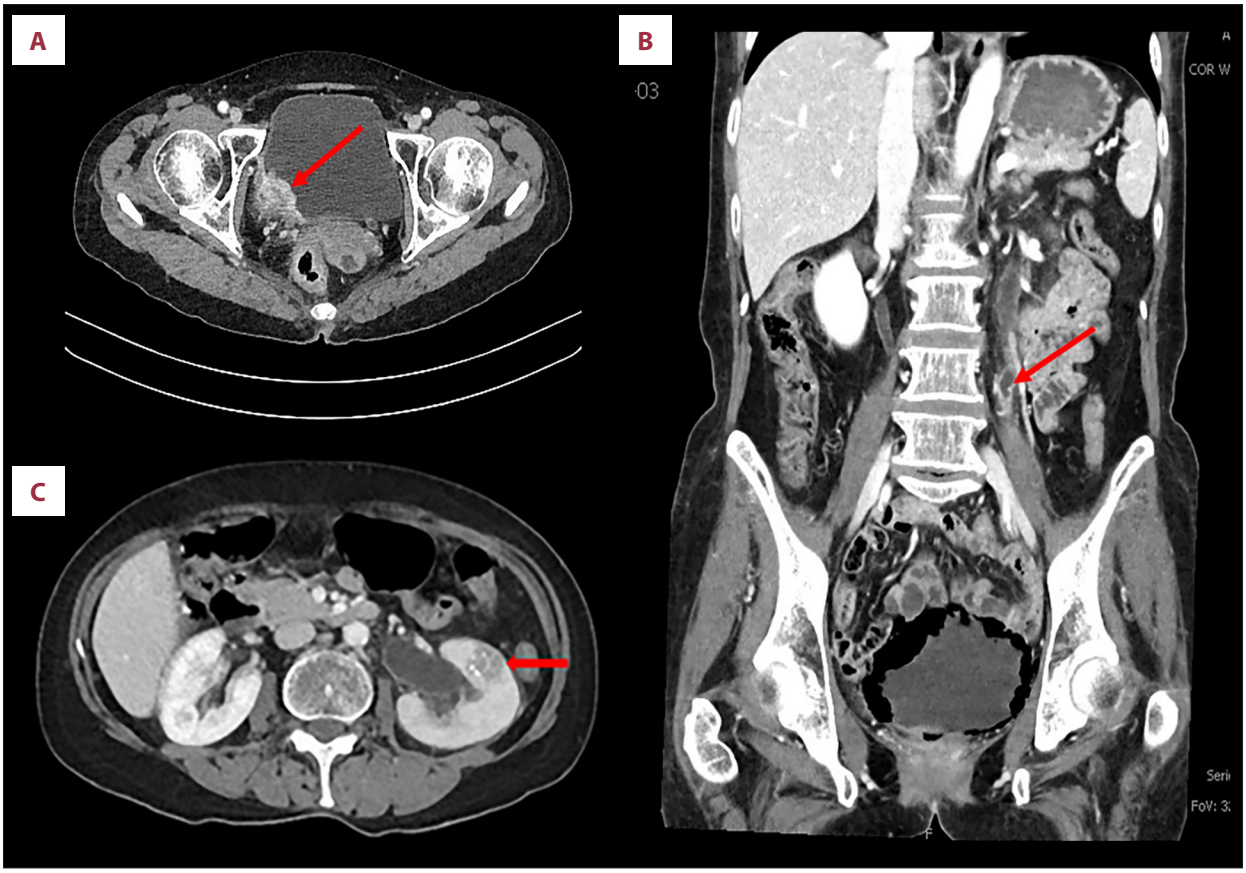


Figure 1. Computed tomography intravenous pyelography. (**A**) Right posterior bladder wall mass (red arrow). (**B**) Left ureteral mass (red arrow). (**C**) Left renal mass (red arrow).

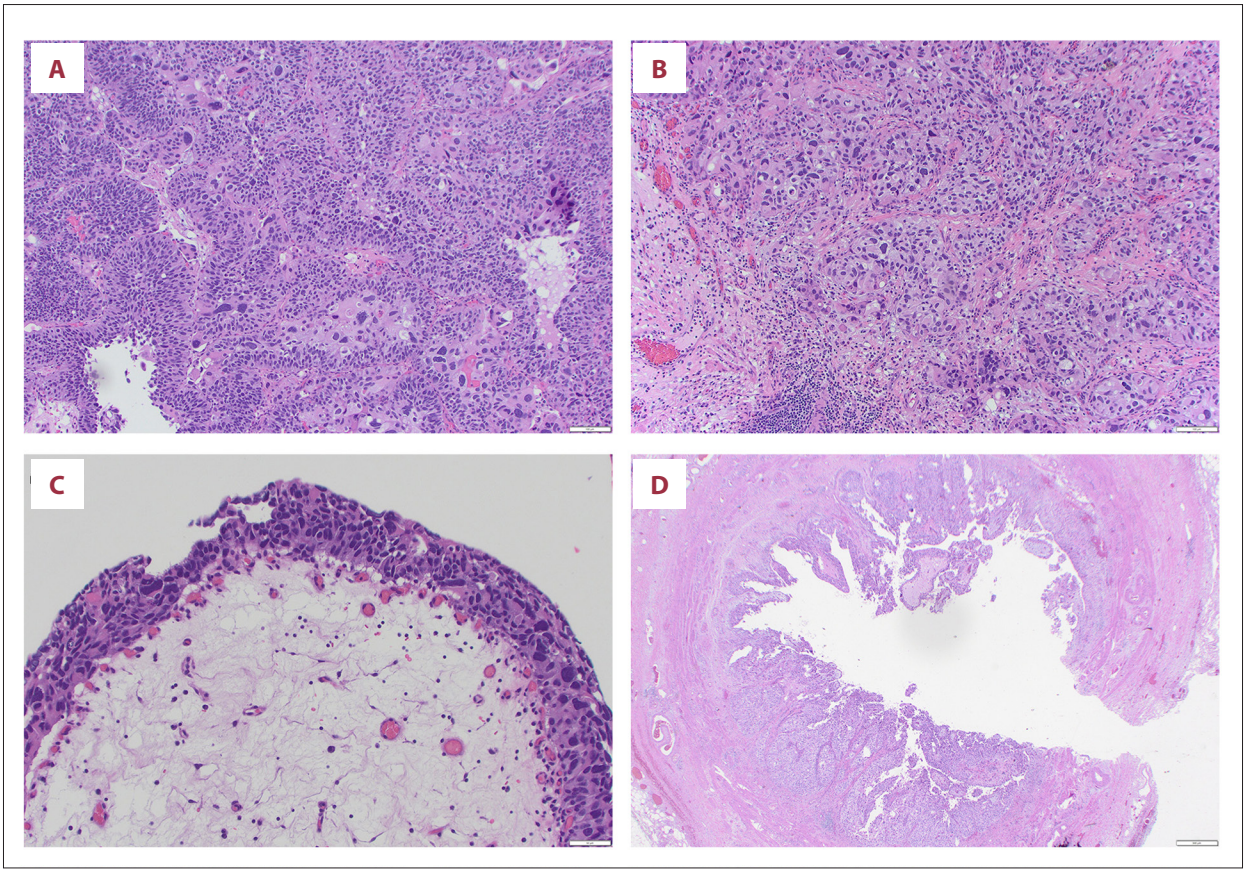
This work is licensed under Creative Commons Attribution-NonCommercial-NoDerivatives 4.0 International (CC BY-NC-ND 4.0)

Indexed in: [PMC] [PubMed] [Emerging Sources Citation Index (ESCI)] [Web of Science by Clarivate]

pyelography revealed 3 distinct masses: a 28-mm lesion in the right posterior bladder wall (**Figure 1A**), a 31-mm lesion in the left mid-ureter (**Figure 1B**), and a 21-mm lesion in the mid to lower pole of the left kidney (**Figure 1C**). Voided urine cytology showed high-grade urothelial carcinoma positivity. Subsequent cystoscopy revealed an 2.8-cm tumor involving the right posterolateral bladder wall, and transurethral resection of the bladder tumor demonstrated high-grade papillary urothelial carcinoma with extensive invasion into the lamina propria (**Figure 2A-2C**). Scant muscularis propria was identified, without signs of malignancy. The left renal pelvis could not be accessed during ureteroscopy because of obstruction by a tumor in the proximal ureter. Concurrent biopsy of the left ureter also revealed high-grade papillary urothelial carcinoma. Based on the diagnosis of high-grade urothelial carcinoma of the ureter, the patient underwent neoadjuvant chemotherapy with 4 cycles of dose-dense methotrexate, vinblastine, doxorubicin, and cisplatin, followed by left nephroureterectomy 4 months after initial presentation.

Gross examination of the nephroureterectomy specimen identified a well-defined, gray-pink, friable renal mass measuring 2.7 × 2.1 × 1.8 cm. The entire tumor was submitted for microscopic evaluation. Microscopically, approximately 90% of the tumor exhibited a biphasic cell population predominantly arranged in acinar structures. The smaller cells, with scant to moderate amounts of eosinophilic granular cytoplasm, were located centrally and formed rosette-like structures surrounding eosinophilic basement membrane-like globules. The larger cells, located peripherally, displayed abundant clear cytoplasm. Occasional papillary, tubular, and clustered structures composed of large clear cells were also observed. Nuclei were relatively uniform, without prominent nucleoli. Numerous psammoma bodies were present (**Figure 3A-3C**). Tumor cells directly invaded the renal sinus fat (**Figure 3D**); however, no invasion of the renal vein or perirenal adipose tissue was identified.

Based on the characteristic morphology, TFEB-rearranged RCC was initially favored. However, subsequent immunohistochemical studies demonstrated that the tumor cells were diffusely positive for paired box 8 (PAX8) and TFE3 (**Figure 3E**); focally positive for human melanoma black 45 (HMB-45; **Figure 3F**); and negative for vimentin, anti-epithelial keratin antibody (AE)1/AE3, carbonic anhydrase IX (CAIX), and Melan-A. In contrast to most conventional RCCs, MiT-RCCs may exhibit reduced expression of epithelial markers, including AE1/AE3, while retaining PAX8 expression. In the present case, diffuse PAX8 expression and the absence of AE1/AE3 expression supported a renal primary tumor and were compatible with the immunophenotype of MiT-RCC. Negative staining for CAIX and vimentin argued against clear



APPROVED GALLEY PROOF

This work is licensed under Creative Commons Attribution-NonCommercial-NoDerivatives 4.0 International (CC BY-NC-ND 4.0)

Indexed in: [PMC] [PubMed] [Emerging Sources Citation Index (ESCI)] [Web of Science by Clarivate]

APPROVED GALLEY PROOF

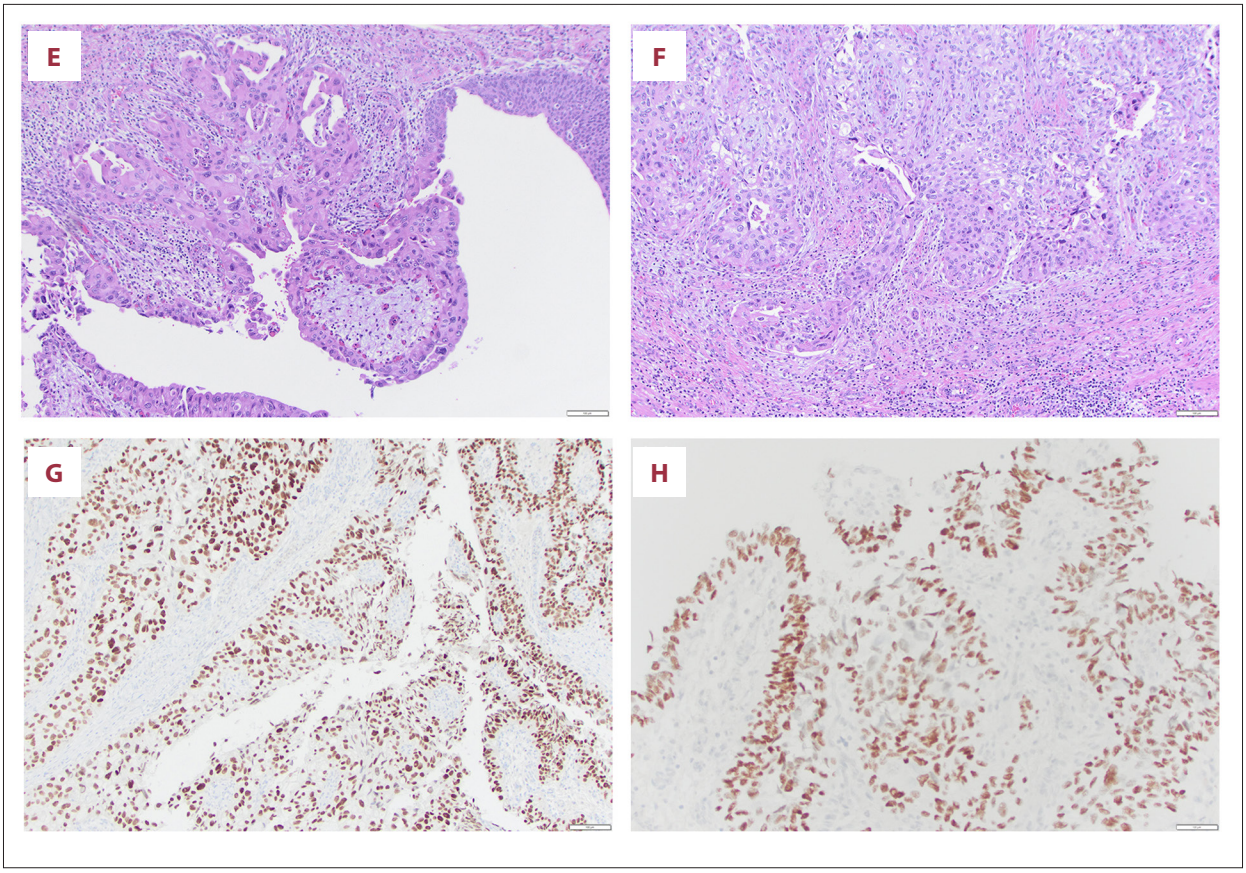


Figure 2. Invasive high-grade urothelial carcinoma of the urinary bladder and left ureter. (A-C) Invasive high-grade urothelial carcinoma of urinary bladder (TURBT specimen). (A) H&E, 100 ×. Tumor cells exhibiting moderate amounts of eosinophilic cytoplasm and enlarged nuclei with pronounced nuclear pleomorphism, irregular nuclear contours, hyperchromasia, and prominent nucleoli. Papillary structures are present. (B) H&E, 100 ×. Tumor cells extensively involving the lamina propria. (C) H&E, 100 ×. Urothelial carcinoma in situ. **(D-H) Invasive high-grade urothelial carcinoma of the left ureter (nephroureterectomy specimen).** (D) H&E, 20 ×. Tumor cells involving the left ureter with focal papillary architecture. (E) H&E, 100 ×. Tumor cells exhibiting morphological features similar to those of the bladder urothelial carcinoma. (F) H&E, 100 ×. Tumor invading the lamina propria. (G) GATA3 IHC, 100 ×. Diffuse nuclear positivity in tumor cells. (H) p63 IHC, 200 ×. Nuclear positivity in the majority of tumor cells. Abbreviations: GATA3, GATA-binding protein 3; H&E, hematoxylin and eosin; IHC, immunohistochemistry; TURBT, transurethral resection of the bladder tumor.

cell RCC and papillary RCC; diffuse TFE3 expression raised the possibility of TFE3-rearranged RCC. However, the morphological features, along with focal positivity of the melanocytic marker HMB-45 and equivocal expression of Melan-A, led us to include TFEB-rearranged RCC in the differential diagnosis. To confirm the diagnosis, both DNA and RNA sequencing were performed. DNA sequencing revealed a tuberous sclerosis complex 1 (TSC1) variant (p.Ile281Lysfs*8); the implications of this alteration in the context of TFE3-rearranged RCC are uncertain (see Discussion). RNA sequencing detected a fusion joining exon 9 of splicing factor proline- and glutamine-rich (SFPQ; also known as polypyrimidine tract-binding protein-associated splicing factor [PSF]) to exon 6 of TFE3. The final diagnosis was SFPQ/PSF-TFE3 RCC.

Invasive high-grade urothelial carcinoma was also confirmed in the ureter within the same nephroureterectomy specimen. The tumor exhibited focal papillary architecture with high-grade nuclear features, including enlarged hyperchromatic nuclei, irregular nuclear contours, prominent nucleoli in some cells, and pronounced nuclear pleomorphism (**Figure 2D, 2E**). The tumor focally invaded the lamina propria (**Figure 2F**), and areas of urothelial carcinoma in situ were present. The urothelial origin was confirmed by diffuse positivity for GATA-binding protein 3 (GATA3) (**Figure 2G**) and p63 (**Figure 2H**), with negative PAX8 staining.

For the high-grade urothelial carcinoma of the urinary bladder, the patient subsequently underwent staged cystectomy with pelvic lymph node dissection and neobladder reconstruction 7 months after initial presentation. The surgical specimen revealed residual multifocal urothelial carcinoma in situ with von Brunn nest involvement.

This work is licensed under Creative Commons Attribution-NonCommercial-NoDerivatives 4.0 International (CC BY-NC-ND 4.0)

Indexed in: [PMC] [PubMed] [Emerging Sources Citation Index (ESCI)] [Web of Science by Clarivate]

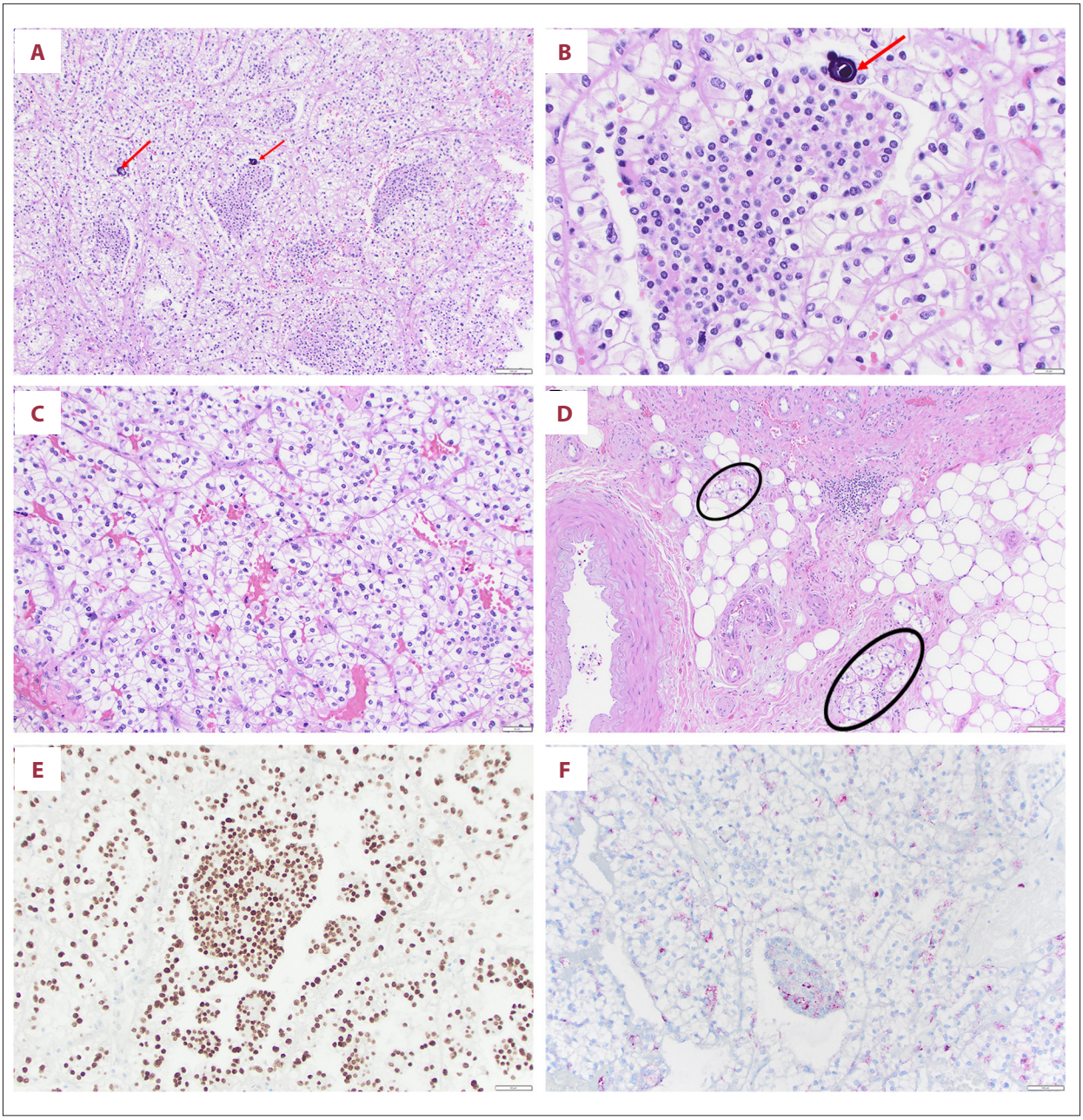


Figure 3. Morphological features and immunohistochemical staining of renal cell carcinoma. (**A, B**) Biphasic growth pattern with acinar structures composed of peripheral large cells with clear cytoplasm and central small cells with eosinophilic cytoplasm surrounding eosinophilic basement membrane-like material. Psammoma bodies are present (red arrows). (**A**) H&E, 100 ×. (**B**) H&E, 400×. (**C**) H&E, 400 ×. Rare areas exhibiting papillary structures composed of clear epithelial cells. (**D**) H&E, 100 ×. Renal sinus fat invasion (black circles). (**E**) TFE3 IHC, 400 ×. Strong, diffuse nuclear positivity in tumor cells. (**F**) HMB-45 IHC, 400 ×. Focal intracytoplasmic positivity. Abbreviations: H&E, hematoxylin and eosin; HMB-45, human melanoma black 45; IHC, immunohistochemistry; TFE3, transcription factor E3.

APPROVED GALLEY PROOF

This work is licensed under Creative Commons Attribution-NonCommercial-NoDerivatives 4.0 International (CC BY-NC-ND 4.0)

Indexed in: [PMC] [PubMed] [Emerging Sources Citation Index (ESCI)] [Web of Science by Clarivate]

APPROVED GALLEY PROOF

The patient has undergone surveillance with chest computed tomography and abdominal/pelvic magnetic resonance imaging every 3 months during the first year and every 4 months during the second year after initial presentation. All scans have shown no evidence of recurrent or metastatic disease through 22 months after initial presentation. Urine cytology performed every 6 months has been negative for high-grade urothelial carcinoma through 23 months after initial presentation. As part of surveillance, the patient has also undergone annual monitoring with a complete blood count, comprehensive metabolic panel, and vitamin B12 testing.

Future chest computed tomography and abdominal/pelvic magnetic resonance imaging scans are planned every 6 months during the third year after initial presentation, annually during the fourth and fifth years, and thereafter as clinically indicated. Urine cytology will also be performed as clinically indicated.

Discussion

TFE3-rearranged RCC was first officially recognized in the 2004 WHO classification of renal tumors, whereas TFEB-rearranged RCC was first officially recognized in the 2013 International Society of Urological Pathology Vancouver classification of renal neoplasia [7]. These 2 subtypes of MiT-RCC share many similarities. Both were initially described in young patients, are relatively more frequent in the pediatric population, and are associated with a worse prognosis in older patients. However, their morphological patterns are considered distinct. TFE3-rearranged RCC typically exhibits a classic triad of papillary architecture, large clear cells with prominent nucleoli, and psammoma bodies. Nevertheless, different fusion partners and breakpoints involving the *TFE3* gene can result in morphological and clinical heterogeneity [8,9]. In contrast, TFEB-rearranged RCC almost always exhibits a biphasic growth pattern with distinctive rosette-like structures. Although biphasic growth patterns have occasionally been detected in TFE3-rearranged RCC [5,10], the rosette-like structures identified in our patient typically favor TFEB-rearranged RCC [6,11].

The TFE3 immunohistochemical stain, which uses an antibody targeting the C-terminal portion of TFE3, is widely used to diagnose TFE3-rearranged RCC, with a sensitivity exceeding 95% [12]. However, false-positive and false-negative results can occur because of variations in fixation and processing conditions [13]. Fluorescence in situ hybridization (FISH) using a TFE3 break-apart probe has generally proven to be more useful because samples are less impacted by fixation issues [3]. Nevertheless, false-negative results can occur in cases of cryptic fusions or intrachromosomal inversions. RNA sequencing—performed in the present case—is a robust technique capable of identifying unexpected TFE3 fusion variants.

Through advances in molecular testing, an increasing number of TFE3 fusion partners and diverse morphological features of TFE3-rearranged RCC have been described. To our knowledge, only Wang et al [14] have reported cases of TFE3-rearranged RCC mimicking TFEB-rearranged RCC. In their study, 2 of 5 cases exhibited rosette-like structures resembling TFEB-rearranged RCC; these occurred in 35- and 36-year-old women. In contrast, our case involved a 66-year-old woman with renal sinus fat invasion (pT3a). In the study by Wang et al, a TFE3 break-apart FISH assay was used to confirm TFE3 rearrangement. Subsequent reverse transcription-polymerase chain reaction demonstrated that 1 of the 2 cases with rosette-like structures harbored an SFPQ exon 9-TFE3 exon 6 fusion, identical to the fusion identified in our case, whereas the other harbored an SFPQ exon 9-TFE3 exon 5 fusion. Wang et al also reviewed 25 previously reported cases of SFPQ/PSF-TFE3 RCC. Most were pT1 or pT2 tumors with papillary structures and subnuclear vacuoles but no rosette-like structures; only 1 was reported as pT4 disease with lymph node metastasis. Argani et al [15] also reported 7 cases of SFPQ/PSF-TFE3 RCC. Morphologically, these tumors exhibited a combination of nested and papillary architectures with predominantly clear cytoplasm. All 7 cases displayed psammomatous calcifications, and 5 showed striking subnuclear vacuoles. None showed morphological features mimicking TFEB-rearranged RCC.

In our case, in addition to the SFPQ/PSF-TFE3 fusion, a TSC1 variant (p.Ile281Lysfs*8) was identified. TSC1 alterations have been reported in various solid tumors, including RCC; to our knowledge, they have not been established as characteristic molecular alterations of translocation RCC. The biological and clinical implications of the TSC1 alteration identified in the present case in the context of TFE3-rearranged RCC remain unclear. Although this alteration could theoretically represent a co-occurring driver or a pathway-relevant event, its potential contribution to tumor development cannot be established based on a single case. Further studies of TFE3-rearranged RCCs with comprehensive molecular profiling are needed to determine whether TSC1 alterations occur repeatedly and have biological or clinical importance.

Along with TFE3-rearranged RCC, our patient had synchronous high-grade urothelial carcinomas involving the bladder and left ureter. Although these tumors occurred concurrently in the same patient, the available morphological and molecular data do not provide evidence of a shared pathogenesis or causal relationship between them. Nevertheless, their coexistence represents a clinically important observation that adds to the diagnostic and therapeutic complexity of the present case.

The limitations of this report include its single-case nature and the limited duration of clinical follow-up, which preclude definitive conclusions regarding long-term prognosis. Given

This work is licensed under Creative Commons Attribution-NonCommercial-NoDerivatives 4.0 International (CC BY-NC-ND 4.0)

Indexed in: [PMC] [PubMed] [Emerging Sources Citation Index (ESCI)] [Web of Science by Clarivate]

that TFE3 break-apart FISH does not identify the fusion partner, we performed RNA sequencing rather than conventional TFE3 break-apart FISH as the confirmatory molecular assay to investigate the relationship between the specific TFE3 fusion partner and the tumor's morphological features. The absence of an additional TFE3 break-apart FISH assay limits the breadth of confirmatory testing; however, it does not negate the RNA sequencing result identifying the SFPQ/PSF-TFE3 fusion. Notably, RNA sequencing is more costly and may not be readily available in routine diagnostic practice.

Overall, our case provides additional evidence supporting and expanding the previously documented morphological spectrum of SFPQ-TFE3 RCC to include extensive TFEB-like features. Our patient was substantially older than the 2 previously reported patients with TFEB-like morphology and had an advanced pathological stage involving renal sinus fat invasion (pT3a). The detailed morphological, immunohistochemical, and molecular characterization in our case provides additional validation of this unusual morphological presentation and adds a further example of its uncommon presentation. Furthermore, the presence of 2 synchronous urologic carcinomas may pose challenges for clinical management, particularly regarding treatment selection and surveillance. Therapeutic regimens and follow-up strategies should be considered in the context of the distinct biological and clinical characteristics of each malignancy.

Conclusions

TFE3-rearranged RCC can occur in older patients and may present as high-stage tumors with morphological features that closely mimic TFEB-rearranged RCC. Although TFE3 immunohistochemistry is a sensitive screening marker, molecular studies may be necessary for definitive classification, particularly when TFE3- and TFEB-rearranged RCCs exhibit overlapping morphological and immunophenotypic features.

Department and Institution Where Work Was Done

University of Colorado, Anschutz Medical Campus, Aurora. CO, USA

Patient Consent

The patient provided informed consent for publication of this report.

Declaration of Figures' Authenticity

All figures submitted have been created by the authors who confirm that the images are original with no duplication and have not been previously published in whole or in part.

References:

1. Argani P, Olgac S, Tickoo SK, et al. Xp11 translocation renal cell carcinoma in adults: Expanded clinical, pathologic, and genetic spectrum. Am J Surg Pathol. 2007;31(8):1149-60
2. Moch H, Humphrey PA, Ulbright TM, Reuter VE, editors. WHO classification of tumours of the urinary system and male genital organs. 4th ed. Lyon: IARC; 2016
3. WHO Classification of Tumours Editorial Board. WHO classification of tumours: urinary and male genital tumours. 5th ed. Lyon: IARC; 2022
4. Calio A, Marletta S, Brunelli M, et al. TFE3 and TFEB-rearranged renal cell carcinomas: An immunohistochemical panel to differentiate from common renal cell neoplasms. Virchows Arch. 2022;481(6):877-91
5. Pei J, Cooper H, Flieder DB, et al. NEAT1-TFE3 and KAT6A-TFE3 renal cell carcinomas, new members of MiT family translocation renal cell carcinoma. Mod Pathol. 2019;32(5):710-16
6. Sharma AE, Parilla M, Wanjari P, Segal JP, Antic T. A tale of 2 morphologies: Diagnostic pitfalls in TFEB-associated renal cell carcinomas, including a novel NEAT1-TFEB fusion. Int J Surg Pathol. 2021;29(1):21-29
7. Srigley JR, Delahunt B, Eble JN, et al. The International Society of Urological Pathology (ISUP) Vancouver classification of renal neoplasia. Am J Surg Pathol. 2013;37(10):1469-89
8. Argani P. MiT family translocation renal cell carcinoma. Semin Diagn Pathol. 2015;32(2):103-13
9. Tretiakova MS. Chameleon TFE3-translocation RCC and how gene partners can change morphology: Accurate diagnosis using contemporary modalities. Adv Anat Pathol. 2022;29(3):131-40
10. Xia T, Long H, Liao D, et al. A case of TFE3 translocation renal cell carcinoma with rare morphological features and literature review. Indian J Pathol Microbiol. 2023;66(1):135-40
11. Argani P, Hawkins A, Griffin CA, et al. A distinctive pediatric renal neoplasm characterized by epithelioid morphology, basement membrane production, focal HMB45 immunoreactivity, and t(6;11)(p21.1;q12) chromosome translocation. Am J Pathol. 2001;158(6):2089-96
12. Argani P, Lal P, Hutchinson B, et al. Aberrant nuclear immunoreactivity for TFE3 in neoplasms with TFE3 gene fusions: A sensitive and specific immunohistochemical assay. Am J Surg Pathol. 2003;27(6):750-61
13. Inamura K. Translocation renal cell carcinoma: An update on clinicopathological and molecular features. Cancers (Basel). 2017;9(9):111
14. Wang XT, Xia QY, Ni H, et al. SFPQ/PSF-TFE3 renal cell carcinoma: A clinicopathologic study emphasizing extended morphology and reviewing the differences between SFPQ-TFE3 RCC and the corresponding mesenchymal neoplasm despite an identical gene fusion. Hum Pathol. 2017;63:190-200
15. Argani P, Zhong M, Reuter VE, et al. TFE3-fusion variant analysis defines specific clinicopathologic associations among Xp11 translocation cancers. Am J Surg Pathol. 2016;40(6):723-37

APPROVED GALLEY PROOF

This work is licensed under Creative Commons Attribution-NonCommercial-NoDerivatives 4.0 International (CC BY-NC-ND 4.0)

Indexed in: [PMC] [PubMed] [Emerging Sources Citation Index (ESCI)] [Web of Science by Clarivate]